SOFT X-RAY INTERFEROMETRY

L. B. Da Silva *J. C. Moreno*

T. W. Barbee, Jr. *J. E. Trebes*

R. Cauble *A. S. Wan*

P. Celliers *F. Weber*

Introduction

In the study of laser-produced plasmas, optical interferometry plays a key role in accurately measuring electron density profiles for a variety of target conditions. Attwood et al.[1] were the first to quantify profile steepening due to radiation pressure using a short pulse 2650-Å optical interferometer. This method was used to measure electron density profiles in exploding foils under conditions relevant to x-ray lasers.[2] Young et al.[3,4] also used optical interferometry to investigate the filamentation instability in laser-produced plasmas. Nevertheless, the size of the plasma and the peak electron density accessible in all these cases were severely restricted by absorption and refraction. Inverse bremsstrahlung absorption becomes significant for optical probes at electron densities exceeding 10^{20} cm^{-3}. Refraction of the probe beam is sensitive to electron density gradients and ultimately affects spatial resolution and data interpretation.[5] These problems are particularly significant as we progress in producing and studying large (3 mm) and high-density (10^{22} cm^{-3}) plasmas relevant to Inertial Confinement Fusion (ICF) and astrophysics. Therefore, we need to develop interferometry techniques at soft x-ray wavelengths where absorption and refraction effects can be mitigated.

This article describes the use of interferometry at soft x-ray wavelengths to probe laser-produced plasma. We discuss the properties and characteristics of existing soft x-ray lasers that make them well suited to probe laser-produced plasma. The design and performance of a multilayer-optic-based interferometer is presented along with results of its use to probe millimeter-size plasmas.

Advantages and Properties of Collisional X-Ray Lasers

Worldwide[6] research demonstrates soft x-ray lasers that operate from 400 to 35 Å (30 to 350 eV). These systems use high-power optical lasers to produce a hot and uniform plasma suitable for laser amplification and propagation. Recently, the efficiency and range of collisionally pumped systems has been increased using multipump pulse techniques.[7] Although recombination schemes have also been used, the highest gain-length products, and consequently output powers, have been observed for neon-like collisionally pumped lasers. Saturated output has been reported in selenium,[8] germanium,[9] and yttrium[10] using optical pumping and in argon using capillary discharges.[11] The high brightness and comparatively routine operation of existing soft x-ray lasers offer an opportunity to use these systems for a variety of applications. These applications include the use of a Ni-like tantalum x-ray laser for biological imaging,[12] which allows us to study biological specimens in a natural environment with resolutions far exceeding those possible with optical techniques. The high brightness of saturated x-ray lasers also makes them an ideal tool for probing high-density and large plasmas relevant to astrophysics and ICF. In addition, the wide range of available x-ray laser wavelengths (Fig. 1) now makes it possible to take advantage of absorption edges to enhance contrast.

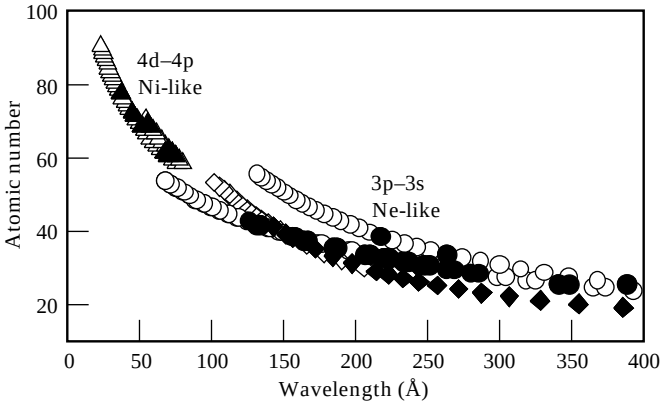

FIGURE 1. Measured (filled symbols) and calculated (open symbols) wavelengths as a function of atomic number for primary neon- (3p–3s) and nickel-like (4d–4p) collisionally pumped x-ray laser lines. (08-00-1295-2637pb01)

This article focuses on the use of soft x-ray lasers to study laser-produced plasmas.

Absorption and Refraction Effects

Two main effects ultimately limit the plasma condition that can be probed with any laser source. The first is absorption, which limits the density of the plasma; the second is refraction, which limits the density gradients. In a plasma with electron density n_e, the index of refraction n_{ref} is related to the critical electron density $n_c = 1.1 \times 10^{21}\ \lambda^{-2}$ (cm^{-3}) (λ in μm) by $n_{ref} = \sqrt{1 - \frac{n_e}{n_c}}$. In an interferometer, the number of fringe shifts, N_{Fringe}, is then given by

$$N_{Fringe} = \frac{\delta\phi}{2\pi} = \frac{1}{\lambda}\int_0^L (1 - n_{ref})\,dl \approx \frac{n_e}{2n_c}\frac{L}{\lambda} = 4.54 \times 10^{-22} n_e L \lambda ,$$

where the integral is along ray trajectories through the plasma. dl is the differential path length, L is the plasma length, and we assume refraction effects are negligible. Experimentally, the maximum number of fringe shifts measurable is usually constrained by detector resolution and is rarely greater than ~50. This imposes a constraint on the product $n_e L$ for a given wavelength. However, absorption is a more significant constraint on the accessible plasma density and size. We can estimate this parameter space by considering only free-free absorption. For most high-temperature plasmas of interest, the level of ionization is sufficient to eliminate any bound-free absorption in the soft x-ray region. Resonant line absorption is possible but very unlikely given the narrow bandwidth (~10 mÅ)[13] of the x-ray laser. Under these conditions the absorption coefficient α is approximately given by[14]

$$\alpha \approx 2.44 \times 10^{-37} \frac{\langle Z^2 \rangle n_e n_i}{\sqrt{T_e}(h\nu)^3}\left[1 - \exp\left(\frac{-h\nu}{T_e}\right)\right] \text{cm}^{-1} . \qquad (1)$$

Here, the electron temperature T_e and photon energy $h\nu$ are in electron volts, and n_e and ion density n_i are in cm^{-3}. The strong scaling with photon energy shows the advantage of probing with soft x-ray sources. Using Eq. (1) if we consider only free-free absorption in a plasma with 1-keV temperature and average ionization of 30 (mid-Z plasma), we obtain $\alpha \approx 2.6 \times 10^{-43}\ n_e^2$ for λ = 155 Å. If we allow for one optical depth (i.e., αL = 1) of absorption, we obtain $n_e^2 L = 3.8 \times 10^{42}$. Figure 2 compares the electron density and plasma dimension accessible with a soft x-ray laser source (155 Å) and an optical laser source (2500 Å). Clearly, the strong wavelength scaling ($\propto \lambda^2$) shows the advantage of probing with shorter wavelengths. The parameter space accessible with a 155-Å probe easily covers the plasmas normally produced in the laboratory.

Refraction of the probe beam is sensitive to electron density gradients and ultimately affects spatial resolution and data interpretation.[5] At 155 Å, $n_c = 4.6 \times 10^{24}$ (cm^{-3}), which is well above that of most plasmas of interest. For a simple plasma with a linear density gradient $n_e = n_0\,[1 - (y/y_0)]$, the deflection angle θ scales as $\theta \propto \lambda^2 L / y_0$. This strong scaling supports the advantage of using a short wavelength probe. Figure 3 compares the deflection angle after propagating through a 3-mm plasma for an optical (2650 Å) and soft x-ray (155 Å) probe source. At a fundamental level, large deflection angles imply significant spatial blurring and reduced spatial resolution. In addition, since probe rays propagate through a range of electron densities, interpretation is more difficult.

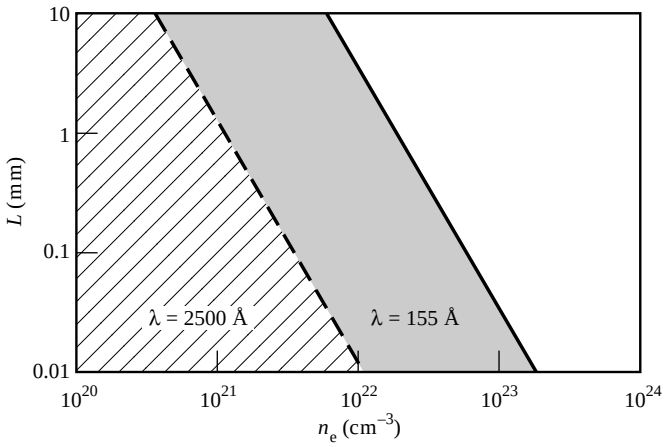

FIGURE 2. Parameter space accessible for plasma probing, using an optical laser (2500 Å) and a soft x-ray laser (155 Å). Only free-free absorption is considered. (08-00-1295-2638pb01)

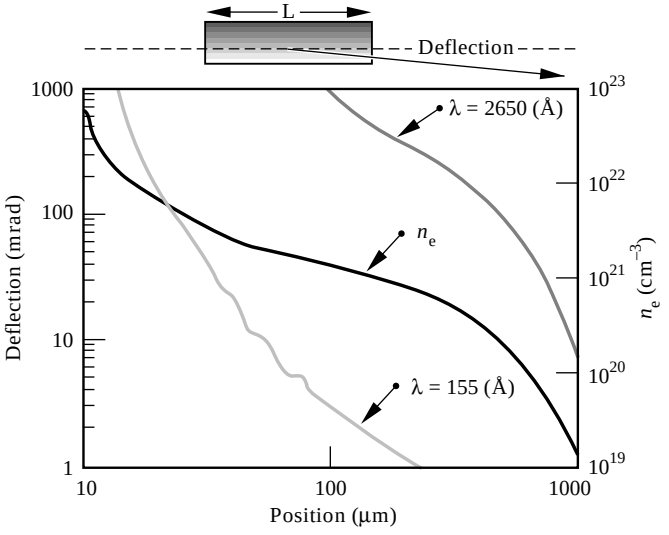

FIGURE 3. Calculated deflection vs path displacement normal to the target surface for an optical (dark gray line) and an x-ray laser (light gray line) probe traversing 3 mm of plasma (produced by driving a 50-μm thick CH target with a 1-ns square 0.53 μm laser pulse at 2.0×10^{13} W/cm^2). The target surface was at 25 μm prior to the pulse. Also shown is the calculated electron density (solid line). (08-00-1295-2639pb02)

The strong wavelength scaling of absorption and refraction ($\propto \lambda^2$) counters the loss in sensitivity caused by the linear scaling of fringe shift with probe wavelength. This difference in scaling makes the soft x-ray regime an attractive area in which to operate. To date, all our experiments for probing plasmas have used the yttrium x-ray laser. This neon-like collisionally pumped x-ray laser is well suited to this application by virtue of its high output power (Fig. 4) and monochromatic output (i.e., dominated by a single line at 155 Å).[10] The wavelength is also well suited to existing multilayer mirror technologies, which have demonstrated reflectivities of ~60%. At Lawrence Livermore

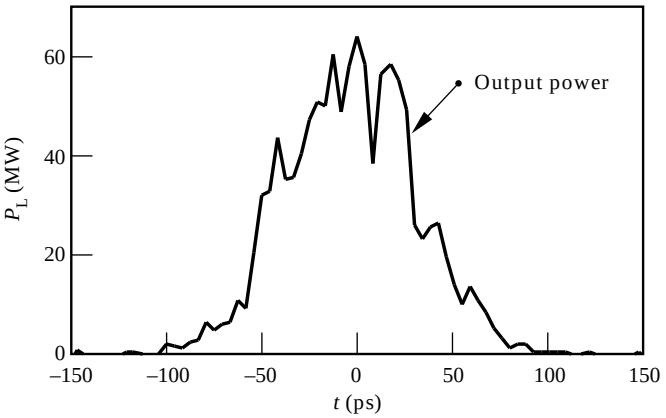

FIGURE 4. Measured output power of 3-cm-long yttrium exploding foil x-ray laser. (08-00-1295-2640pb01)

National Laboratory (LLNL), we use this system to image accelerated foils[15] and measure electron density profiles in a laser irradiated target using moiré deflectometry.[16] More importantly, we have developed the necessary technology to perform x-ray laser interferometry. In contrast to other techniques, interferometry offers the possibility of directly measuring the two-dimensional (2-D) electron density profile.

Interferometry Using Soft X-Ray Lasers

Extending conventional interferometric techniques into the soft x-ray range has been difficult because of the problems with designing optical systems that operate in the range of 40–400 Å. Reflective / grating systems have been used successfully at 1246 Å.[17] Svatos et al.[18] have demonstrated a purely reflective Fresnel bimirror setup at 48 Å. Both techniques, however, lack some of the advantages of standard interferometer geometries. Fortunately, multilayer mirror technology now allows us to have artificial structures that can be routinely fabricated with reflectivities as high as 65% at 130 Å[19] and with the overall uniformities required by more conventional interferometers.

Figure 5 is a schematic of the experimental setup used to probe plasmas. The system consists of a collimated x-ray laser source, an imaging mirror, and an interferometer. For our experiments, we chose to employ a skewed Mach–Zehnder interferometer, consisting of two flat multilayer mirrors and two multilayer beamsplitters (the most critical element in the system). The polarizing properties of multilayer mirrors, when operated at 45°, prevented us from using a more conventional Mach–Zehnder geometry. Each multilayer mirror consisted of a superpolished (<1 Å rms roughness) fused silica blank coated with 30 layer pairs of Si at 55.9 Å and Mo at 23.9 Å. The mirrors had a peak reflectivity of 60 ±5% at 155 Å. Although soft x-ray beamsplitters with small apertures have previously been used in x-ray laser cavities,[20] comparatively large open areas were necessary for our application. The *active* region of the beamsplitters used in the interferometer was 1.2×1.2 cm and consisted of 1000 Å of Si_3N_4 overcoated with 8 to 12 layer pairs of Mo / Si. The beamsplitters were fabricated from polished Si wafers overcoated with 1000 Å of Si_3N_4. The Si substrate thickness was varied from 0.4–0.8 mm, with the best results at thicker samples. The coated wafers were annealed to achieve maximum tension in the Si_3N_4. Anisotropic Si etching techniques were used to remove the Si substrate from a 1.2- × 1.2-cm area. The flatness

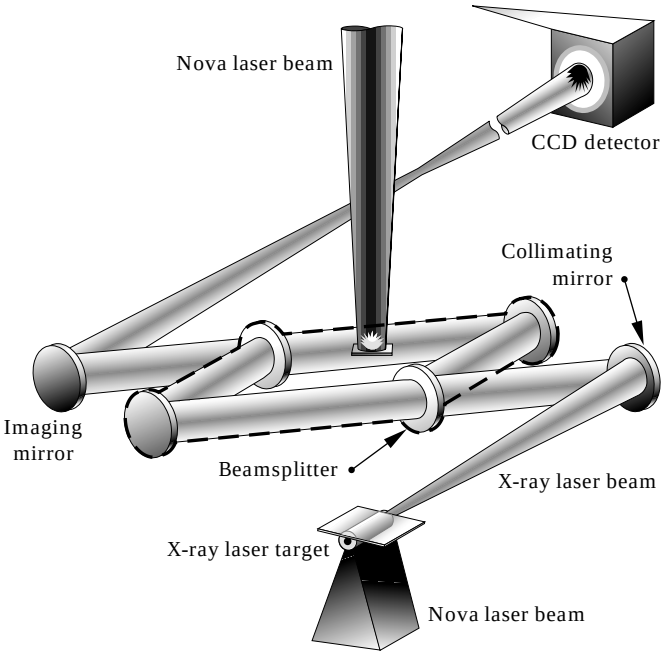

FIGURE 5. Experimental setup showing the optical components for plasma probing using a soft x-ray Mach–Zehnder interferometer. (08-00-1295-2641pb01)

of the beamsplitters was subsequently measured with an optical interferometer. Over the clear aperture, the figure error was typically less than 5000 Å for high-quality Si substrates but could be significantly worse (10000 Å) for conventional thin (0.4 mm) Si wafers. The figure quality was also extremely sensitive to the tension of the Si_3N_4 membrane. The best results were obtained with high-stress membranes (~200 MPa), which had a manufacturing yield of approximately 30%. The measured reflectivity and transmission for these beamsplitters at 155 Å were 20% and 15%, respectively. The overall throughput of each arm, accounting for the mirror and beamsplitter (one transmission and one reflection), was $\sim 0.6 \times 0.20 \times 0.15 = 0.018$.

The probe source consisted of a collisionally pumped neon-like yttrium x-ray laser, operating at 155 Å. The x-ray laser was produced by irradiating a solid 3-cm-long yttrium target with one beam from Nova (λ_{laser} = 0.53 µm, 600 ps square) at an intensity of 1.5×10^{14} W/cm^2. In this pumping geometry, the x-ray laser has an output energy of 3 ±2 mJ, a divergence of approximately 10–15 mrad (FWHM), and an output pulse width of 250 ps. The short pulse width allowed us to obtain an interferogram in a single 250-ps exposure, thereby reducing the effects of vibrations. A spherical multilayer mirror, placed 50 cm from the x-ray laser, collimated the beam and injected it into the interferometer. The transverse coherence length, after beam collimation, was calculated to be $L_s \approx 50$–100 µm, and the longitudinal coherence length was measured to be $L_t \approx 150$ µm. The limited transverse and longitudinal coherence constrains us to match the two paths of the interferometer to maximize fringe visibility. The interferometer was prealigned on an optical bench, using a 200-µm optical fiber and a white light source. Observation of white light fringes matched the optical path lengths to better than 2 µm.

The plasma to be probed was imaged onto a charge-coupled device (CCD) using a 100-cm radius of curvature multilayer mirror with an effective *f* number of 25. The CCD was a back illuminated TEK1024B with 1024×1024 24-µm pixels and a measured quantum efficiency of 40 ±10% at 155 Å. A filter consisting of 1000 Å of Al and 2000 Å of lexan directly in front of the CCD eliminated stray optical light. To reduce background self-emission, a series of three multilayer mirrors reduced the bandpass of the system. The effective bandpass of this system was 4 Å, which is significantly broader than the 10-mÅ spectral width of the x-ray laser source. The image magnification was 19, giving a pixel limited resolution of ~1.3 µm. Figure 6 shows a typical interferogram obtained using this system. In this figure, there is no target plasma; the dark band is an alignment reference positioned at the object plane of the imaging optic. Analysis of the fringe pattern gives a maximum figure error of 300 Å over the full 3-mm field of view and a fringe visibility of 0.7 ±0.2.

Figure 7 shows the interferogram of a plasma produced by irradiating a Si wafer overcoated with 10 µm of CH. The triangular shaped target allows a range of plasma lengths to be probed simultaneously. The Si substrate was polished to ~7 Å rms roughness to

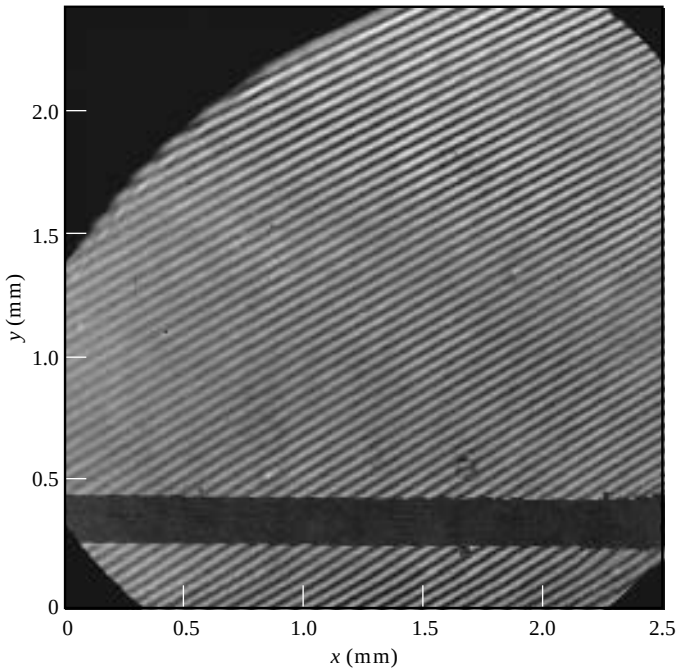

FIGURE 6. Soft x-ray (155 Å) interferogram showing a fringe visibility better than 0.5. The horizontal bar is an alignment reference at the object plane. (08-00-1295-2642pb01)

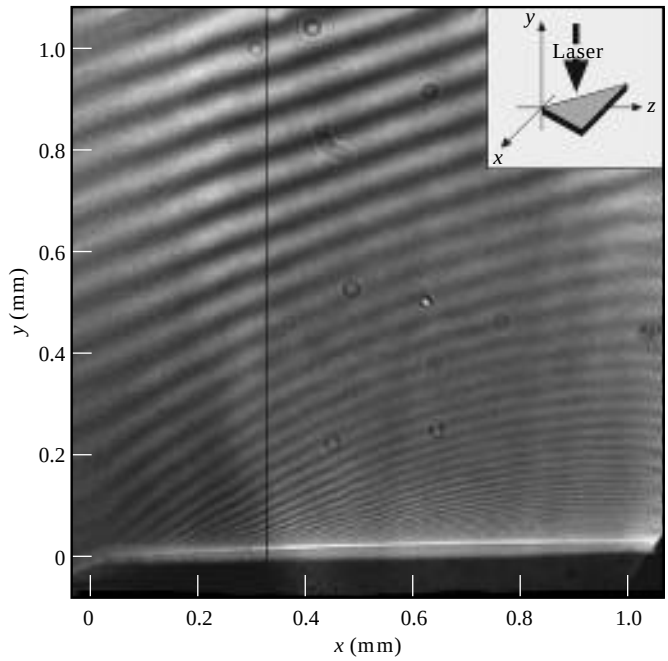

FIGURE 7. Interferogram of CH target irradiated at 2.7×10^{13} W/cm^2. The vertical line shows the position of the lineout in Fig. 8. The inset shows the target geometry. (08-00-1295-2643pb01)

produce a clean flat surface. The CH side was irradiated by a beam smoothed with random phase plates (RPPs) and segmented with wedges to produce a flat-top intensity distribution over a 0.7-mm-diam spot.[21] A 1-ns square laser pulse with a wavelength of 0.53 μm produced an intensity on target of 2.7×10^{13} W/cm^2. The target was backlit edge-on by the x-ray laser beam 1.1 ns after the start of the laser pulse. The image shows excellent fringe visibility and very little self emission from the plasma.

Figure 8 shows the measured electron density as calculated from the interferogram at a distance of 0.35 mm from the tip of the target where the probe length is 0.7 mm. Fringes are clearly resolved as close as 0.025 mm from the initial target surface. The fast evolution of the density profile, close to the critical surface, causes motion blurring of the fringes within the 250-ps x-ray laser frame time. Figure 8 also shows the calculated electron density profiles obtained from a one-dimensional (1-D) LASNEX simulation. The simulation results predict higher electron densities than measured with the discrepancy, increasing as we move away from the surface. This trend is consistent with the plasma expansion not being 1-D, which leads to significant lateral expansion and lower electron densities. We chose a triangular target geometry to illustrate the range of plasma lengths that can be easily probed with a soft x-ray laser. Unfortunately this geometry leads to a three-dimensional expansion, which is difficult to simulate. In the near term, we plan to improve both the target geometry and laser uniformity to generate a truly 2-D profile, which can be accurately compared with simulations. However, the magnitude of the discrepancy we observe between the experiment and simulations is similar to that measured using soft x-ray deflectometry.[16]

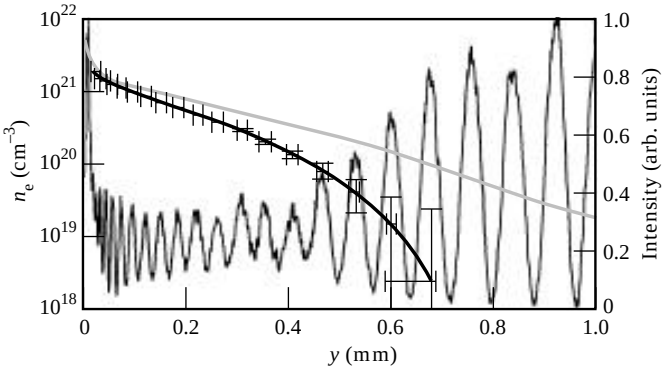

FIGURE 8. The thin solid line is a lineout through the interferogram of Fig. 7 at a position x = 0.35 mm. The thick solid line shows the calculated electron density profile and estimated error bars. The gray line is the electron density profile as calculated by one-dimensional LASNEX simulation. (08-00-1295-2644pb01)

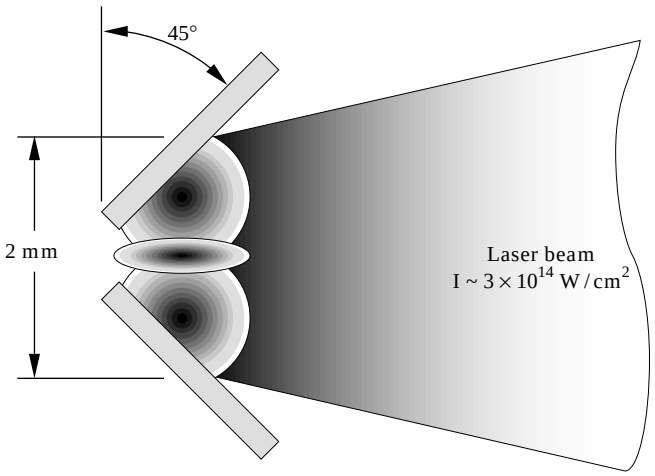

FIGURE 9. Target geometry for studying colliding plasmas. (08-00-1295-2645pb01)

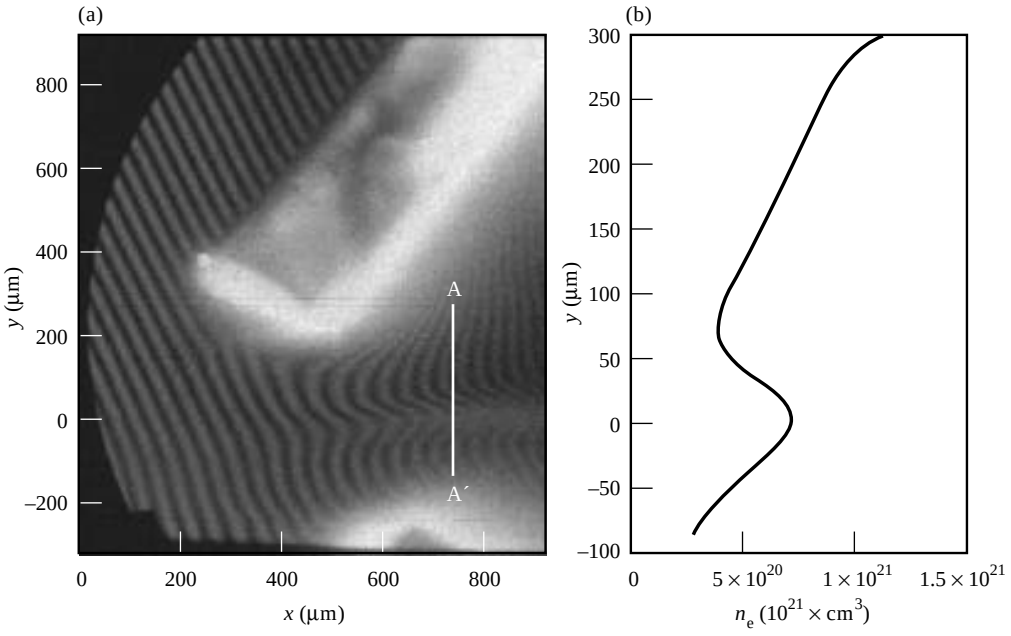

FIGURE 10. (a) Interferogram obtained of Au colliding plasma. (b) Electron density calculated from interferogram along line A–A'. (08-00-1295-2646pb01)

More recently, we used this interferometer to probe colliding plasmas that have relevance in ICF hohlraum experiments. The target consisted of two pieces of 3- × 2-mm polished Si, which were coated with 2 μm of Au and positioned as shown in Fig. 9. The target was irradiated at an intensity of 3×10^{14} W / cm^2 (λ_{laser} = 0.53 μm, 1 ns square), with a focal spot 2 mm high and 0.5 mm wide produced by combining cylinder lenses and RPPs. Figure 10 shows an interferogram at a time 1.0 ns after the start of the drive—providing clear evidence of interpenetrating plasmas. Figure 10(b) shows the measured electron density profile along the line A–A' in Fig. 10(a). The region of plasma stagnation and interpenetration is ~100 μm, which is larger than predicted by simple fluid codes. We are currently modeling this experiment, and we plan to publish the results in the future.

Conclusion

The high brightness and short wavelength of x-ray lasers make them ideally suited for studying long scalelength and high-density plasmas. Our results illustrate the importance of soft x-ray interferometry in diagnosing laser-produced plasmas by reducing the effects of absorption and refraction. Detailed comparisons of 2-D electron density profiles obtained from the x-ray laser interferogram and profiles obtained from radiation hydrodynamics codes, such as LASNEX, will allow us to study the physics of laser–plasma interactions in more detail. Ultimately, our motivation for developing x-ray laser interferometry is to provide a mechanism to probe the deficiencies of our numerical models in areas such as laser deposition by both resonance and inverse bremsstrahlung absorption, flux-limited heat conduction, hydrodynamics, and non-LTE (local thermodynamic equilibrium) atomic kinetics. In the near future, this technique will be used to diagnose the plasmas produced in ICF hohlraum targets, which has been impossible with conventional optical interferometry. In addition to probing laboratory plasmas, an x-ray interferometer can be used to characterize the figure and phase properties of multilayer mirrors near the intended operating wavelength. Measurement of spectral lineshapes with unprecedented resolution is also possible.[17,22]

Notes and References

1. D. T. Attwood, D. W. Sweeney, J. M. Auerbach, and P. H. Y. Lee, *Phys. Rev. Lett.* 40, 184–186 (1978).
2. M. D. Rosen, P. L. Hagelstein, D. L. Matthews, E. M. Campbell, et al., *Phys. Rev. Lett.* 54, 106 (1985); G. Charatis, G. E. Busch, C. L. Shepard, P. M. Campbell, and M. D. Rosen, *Journal De Physique* C6, 89 (1986); M. K. Prasad, K. G. Estabrook, J. A. Harte, R. S. Craxton, *Phys. Fluids B* 4, 1569 (1992).
3. P. E. Young, *Phys. Fluids B* 3, 2331–2336 (1991).
4. S. Wilks, P. E. Young, J. Hammer, M. Tabak, and W. L. Kruer, *Phys. Rev. Lett.* 73, 2994–2997 (1994).
5. L. B. Da Silva, B. Cauble, G. Freiders, J. A. Koch, et al., (SPIE–International Society for Optical Engineering, Bellingham, WA, 1994; *Proc. SPIE* 2012, 158).
6. *X-Ray Lasers 1994* , D. C. Eder, and D. L. Matthews, Eds., (American Institute of Physics, Williamsburg, VA, 1994) vol. 332; *X-Ray Lasers 1992*, E. E. Fill, Ed., (IOP Publishing Ltd, Schliersee, Germany, 1992) vol. 125.
7. H. Daido, R. Kodama, et al., *Opt. Lett.* 20, 61–63 (1995); L. B. Da Silva, R. A. London, B. J. MacGowan, S. Mrowka, et al., *Opt. Lett.* 19, 1532–1534 (1994); J. Nilsen, B. J. MacGowan, L. B. Da Silva, and J. C. Moreno, *Phys. Rev. A* 48, 4682–4685 (1993). E. E. Fill, Y. L. Li, G. Preztler, D. Schlogl, et al., *Physica Scripta* 52, 158–161 (1995); T. Hara, K. Ando, and Y. Aoyagi, *AIP Conference Proceedings* 332, 181–185 (1995).
8. B. J. MacGowan, L. B. Da Silva, D. J. Fields, C. J. Keane, et al., *Phys. Fluids* 4, 2326–2337 (1992).
9. A. Carillon, H. Z. Chen, P. Dhez, L. Dwivedi, et al., *Phys. Rev. Lett.* 68, 2917–2920 (1992).
10. L. B. Da Silva, B. J. MacGowan, S. Mrowka, J. A. Koch, et al., *Opt. Lett.* 18, 1174–1176 (1993).
11. J. J. Rocca, V. Shlyaptsev, F. G. Tomasel, O. D. Cortazar, et al., *Phys. Rev. Lett.* 75, 1236–1236 (1995) and *Phys. Rev. Lett.* 73, 2192–2195 (1994).
12. L. B. Da Silva, J. E. Trebes, R. Balhorn, S. Mrowka, et al., *Science* 258, 269–271 (1992).
13. C. W. Allen, *Astrophysical Quantities*, (Oxford University Press, New York, NY 1963).
14. J. Koch, B. J. MacGowan, L. B. Da Silva, D. L. Matthews, et al., *Phys. Rev. Lett.* 68, 3291 (1992).
15. R. Cauble, L. B. Da Silva, T. W. Barbee, P. Celliers, et al., *Phys. Rev. Lett.* 74, 3816–3819 (1995).
16. D. Ress, L. B. Da Silva, R. A. London, J. E. Trebes, et al., *Science* 265, 514–517 (1994).
17. S. Chakrabarti, D. M. Cotton, J. S. Vickers, and B. C. Bush, *Appl. Opt.* 33, 2596–2602 (1994).
18. J. Svatos, D. Joyeux, D. Phalippou, and F. Polack, *Opt. Lett.* 18, 1367–1369 (1993).
19. T. W. Barbee Jr., J. C. Rife, W. R. Hunter, M. P. Kowalski, et al., *Appl. Opt.* 32, 4852–4854 (1993); D. G. Stearns, R. S. Rosen, and S. P. Vernon, *J. Vac. Sci. Technol. A, Vac. Surf. Films* 9, 2662–2669 (1991).
20. A. M. Hawryluk, N. M. Ceglio, D. G. Stearns, K. Danzmann, et al., (SPIE–International Society for Optical Engineering, Bellingham, WA, 1987; *Proc. SPIE* 688, 81–90).
21. S. G. Glendinning, S. V. Wever, P. Bell, L. B. Da Silva, et al., *Phys. Rev. Lett.* 69, 1201–1204 (1992).
22. M. R. Howells, K. Frank, Z. Hussain, E. J. Moler, et al., *Toward a Soft X-Ray Fourier Transform Spectrometer*, LBL-34798, (1993).